

Expected effects of hot CCD pixels on detection of transits of extra-solar planets with the *Kepler Mission*

Thomas N. Gautier^{*a} and Ronald Gilliland^b

^aJet Propulsion Laboratory, California Institute of Technology, 4800 Oak Grove Drive, Pasadena, California 91109

^bSpace Telescope Science Institute, 3700 San Martin Dr., Baltimore, MD 21218

ABSTRACT

Detection of Earth sized extra-solar planets by the transit method requires measurement of quite small variations ($\sim 8 \times 10^{-5}$) in the brightness of candidate stars. Noise contributed by hot pixels in CCD detectors operating in the space environment, among other noise sources, must be understood and controlled in order to design transit experiments like the *Kepler Mission*, which will attempt to measure the distribution of planets as small as the Earth around solar type stars from space. We have analyzed the hot pixel statistics for CCD detectors on several operating space instruments and conclude that neither the amplitude nor the variability of hot pixels will significantly impair the ability of the *Kepler Mission* to detect transits of earth sized planets transiting solar type stars. The *Kepler Mission* is currently in the design stage and is expected to begin operation in 2007.

Keywords: extra-solar planets, planet detection, photometry, CCDs, space observatories, transit method, Kepler Mission, hot pixels

1. INTRODUCTION

The *Kepler Mission* is a NASA Discovery mission that will search for extra-solar planets with the technique of transit detection. Kepler is currently under development by NASA Ames Research Center, the Jet Propulsion Laboratory, the Space Telescope Science Institute, Ball Aerospace and Technologies Corporation and Honeywell and expects to launch in 2007. The transit technique for planet detection finds planets by recognizing the slight dimming of the planet's parent star as the planet passes in front of the star as seen from Earth. Kepler is being designed to find Earth sized planets around solar like stars so it must achieve extraordinarily high sensitivity to reliably detect the 86 parts per million change in brightness caused by these transits. Planets in 1 year orbits around solar like stars will have transit durations up to about 13 hours. Photometric techniques to achieve this sensitivity have been developed and demonstrated under laboratory conditions¹.

Operation in space exposes CCD detectors, like those Kepler will use, to energetic particle radiation which produces noise sources that were not all simulated in the laboratory demonstration. Energetic particles, primarily high energy solar wind protons in the case of Kepler, produce several noise generating effects in CCD detectors. The primary, but short term effect, is to deposit a large amount of charge in the CCD along the path of a particle passing through the detector. The part of this charge collected by the photoelectron collection and transfer structures of the CCD produces a spike of charge for the length of one readout and may produce lower levels of signal for some number of subsequent readouts if the initial charge deposition is sufficient to produce a significant number of trapped carriers. Secondary effects are due to damage to the silicon lattice of the CCD and can produce centers of excess dark current, traps that reduce charge transfer efficiency (CTE) and potentially other effects as well. CTE degradation is fairly well understood. Instantaneous spikes were included in the laboratory demonstration¹. The focus of this paper is noise produced by the secondary effect of increased dark current centers, otherwise known as hot pixels or dark spikes, which is not as well understood and was not included in the laboratory tests.

The Kepler CCDs are not yet available for testing so no hot pixel measurements of Kepler detectors are available. Therefore, we have used in-flight data from CCDs in existing Hubble Space Telescope (HST) instruments, the High Resolution Camera in the Advanced Camera for Surveys (ACS/HRC), the Space Telescope Imaging Spectrometer (STIS), and the Wide Field/Planetary Camera 2 (WFPC2), to develop a model of hot pixel behavior for

* Thomas.N.Gautier@jpl.nasa.gov; phone 818 354-7204

the Kepler detectors. After a brief explanation of how Kepler will collect its data and a comparison of the CCDs and radiation environment of Kepler to those of the HST instruments we will detail the results of our analysis of the HST data and discuss the predicted effects of hot pixels on transit detections with Kepler.

1.1 Kepler Data Collection and Transit Identification

The Kepler flight system will use a 0.95m aperture Schmidt camera to image 100 deg² of sky onto an array of 42 2Kx1K CCDs. Small sub-arrays of about 32 pixels will be selected around each of about 100,000 target stars in each exposure and these pixels, along with special calibration pixels will be sent to the ground for processing and transit detection. Several short exposures of the selected pixels will be coadded on board the flight system to produce sampling of the target stars' brightness with a 15 minute period. Kepler will stare at the same point on the sky and sample the same target stars every 15 minutes for 4 years. A signature of true planetary transits will be that all pixels within a target star's sub-array will participate in the transit dimming proportionally, keeping the photocenter of the sub-array at a constant location on the sky. This and other features of true transits, such as absolute periodicity of transit repetition and uniform transit depth will be used to eliminate noise induced "pseudo transits" during ground data processing. Further details of the experiment design of Kepler can be found in the references^{2,3,4}.

1.2 CCD Characteristics and Radiation Environments of Kepler and HST

The CCD detectors in the HST ACS/HRC and in STIS are nominally identical and are quite similar to the Kepler CCDs. We expect that the behavior of the HST detectors can be scaled by detector area to predict the behavior of the Kepler arrays. Table 1 details the characteristics of the Kepler and HST detectors. The Kepler detectors are very comparable to the STIS and ACS/HRC detectors in most important respects except the manufacturer. (The difference between the 3 phase and 4 phase collection structures is not expected to make a difference in hot pixel performance.) Ball Aerospace has now had extensive experience with CCDs from both SITE and E2V and expects that the Kepler E2V CCDs will be no worse behaved than the HST SITE arrays⁵. With similar radiation exposure, discussed below, the hot pixel behavior of the HST arrays should be scalable by area and operating temperature to predict the hot pixel behavior of the Kepler arrays. The WFPC2 CCDs are rather different from the Kepler detectors and are difficult to use as convincing models for Kepler. The WFPC2 hot pixel data was analyzed to give additional general indications of expected behavior of the Kepler arrays but was not used to model Kepler performance.

| | Kepler | ACS/HRC | STIS | WFPC2 |
|----------------------------|--|--|--|------------------------------------|
| Manufacturer | E2V | SITe | SITe | Loral Aerospace |
| Pixel Size | 27 μm | 21 μm | 21 μm | 17 μm |
| Size | 2200x1044 | 1024x1024 | 1024x1024 | 800x800 |
| Architecture | Thinned, backside illuminated, 4 phase | Thinned, backside illuminated, 3 phase | Thinned, backside illuminated, 3 phase | Front side illuminated, 3 phase |
| Epilayer thickness | 16 μm | 13-16 μm | 13-15 μm | |
| Depletion depth | 5 μm effective | ~7 μm | ~7 μm | |
| Operating temp | -93C | -81C | -83C | -85C |
| Normal Dark current | | 0.005 e-/s | 0.003 e-/s | ~0.004 e-/s |

Table 1. Characteristics of HST and Kepler CCD detector arrays.

Hot pixels are thought to arise in CCDs when a center of displacement damage in the silicon lattice is present in a region of high electric field strength and the resulting current can be collected by the transfer structures in the CCD. Displacement damage in the silicon crystal is due to non-ionizing energy loss (NIEL) and the total displacement damage dose (DDD) is proportional to the integral of the NIEL. For similar geometries, as is the case between Kepler and ACS/HRC and STIS, hot pixel numbers should be proportional to the displacement damage dose with little or no dependence on dose rate⁶. A rather complete sector analysis of radiation shielding and a careful calculation of the resulting DDD was done for Kepler⁷ yielding a prediction of 5.6x10⁶ MeV/g(Si) per year (1x radiation dose multiplier, 95% confidence level for solar storms and averaged over the 4 year mission life). No such careful analysis is available

for the HST instruments. The shielding sector analyses for ACS only set a lower limit of 0.95-1.0 inch equivalent of aluminum over >99% of 4π steradians^{8,9}. The ACS group calculated a DDD for the ACS Wide Field Camera CCD of 5.2×10^6 MeV/g(Si) per year based on 1 inch equivalent Al and the expected radiation environment of HST¹⁰. This dose can be assumed to apply to ACS/HRC as well since its shielding analysis also set a lower limit of 1 inch Al.

Since 1 inch equivalent Al is the lower limit of the HRC shielding the predicted DDD is not directly comparable to the DDD predicted for Kepler and an estimate must be made of a more realistic DDD for HRC. Dale, *et al.*¹¹, present results of actual tests of the shielding efficiency of aluminum against protons with the energy spectra expected in environments comparable to that of HST. Their shielding efficiency figures 4-7 indicate that a factor of 10 or more increase in shielding thickness over 1 inch equivalent Al only reduces the DDD by a factor of about 3, a conservative compromise, for the HST orbit, between the efficiencies shown against solar flare protons and trapped protons. A factor of 3 reduction in predicted DDD for ACS/HRC to 1.7×10^6 MeV/g(Si) per year should be a lower limit to the HRC DDD since only a few more equivalent inches Al shielding is available in the ACS structure and the aft shroud of the HST.

Another technique using a relation between DDD and CTE degradation, also developed in the Dale, *et al.*, paper¹¹, and the measured CTE degradation of the STIS CCD¹² yields a DDD of 1.2×10^6 MeV/g(Si) per year. We will adopt the value of 1.7×10^6 MeV/g(Si) per year for ACS/HRC putting its DDD a factor of 3.3 below the prediction for Kepler.

2. METHODOLOGY

The Ball Aerospace model for Kepler performance indicates that Kepler will collect about 1.97×10^5 photoelectrons per second from an $m_v=12$, G2V star. The basic noise requirement on the Kepler photometer is that the transit of an earth sized planet in a 1 year orbit across this star, which produces a dimming of 86 parts per million for a grazing transit of about 6.5 hours, be detected with a signal to noise ratio of 4. This sets the 1σ noise level at 6.8×10^4 e⁻ for 6.5 hr integration time.

Shot noise from HST hot pixels is negligible to Kepler. The hottest pixel seen was about 60 e⁻/s in the ACS/HRC and about 15 e⁻/s in WFPC2. STIS data saturates above about 32 e⁻/s but the histograms below do not indicate that dark currents much greater than 60 e⁻/s were present. The shot noise of 60 e⁻/s integrated over 6.5 hr is 1.2×10^3 e⁻ and is totally negligible. A pixel has to be hotter than 4×10^4 e⁻/s to increase the shot noise of an $m_v=12$ G2V star by 10%.

Only actual variability in hot pixel current can effect Kepler noise. Twenty parts per million of 1.97×10^5 is 4 e⁻/s so only pixels hotter than about 2 e⁻/s are of interest because full on to off variation of this magnitude of dark current can introduce as much as 0.5 sigma extra noise. Accordingly we selected all pixels hotter than 2 e⁻/s from the HST data and analyzed their variability. For each time series of hot pixels measurements between anneals we compiled statistics of the total number of pixels hotter than 2 e⁻/s and the number of pixels with peak to peak variation or maximum magnitude of change between adjacent samples larger than 2 e⁻/s. Additionally, in the case of ACS/HRC where the time resolution of the dark images was high, we ran a crude transit filter along all time series for each pixel to look for variations that could mimic a planetary transit. We will argue that the number of troublesome hot pixels and false transits will be negligibly small in the Kepler data.

3. HOT PIXEL DATA

3.1 ACS/HRC and STIS

The HST instruments maintain historical hot pixel data for calibration purposes. The ACS/HRC and STIS archive "superdark" images that give the dark current of all pixels in the arrays and flag pixels designated as "hot". STIS updates its superdarks on a weekly basis with individual dark exposures made twice daily while ACS/HRC updates daily based on 4 dark exposures each day. The details of hot pixel recognition differ slightly between the two instruments but the process basically looks at the distribution of dark currents over the arrays and declares pixels hot if they show dark currents more than 5σ above the median or σ trimmed mean of the array. This results in pixels being declared hot if their dark current exceeds about 0.008 e⁻/s. Many thousands of hot pixels are flagged in each superdark but, as discussed below, only about 5% of the flagged pixels are hot enough to be of interest to Kepler. The exposure time and the gain setting used for the ACS/HRC dark data leads to significant saturation effects for pixels hotter than about 130 e⁻/s. The hottest pixels seen in the ACS/HRC show about 60 e⁻/s so the HRC data should be free of saturation effects. The STIS dark exposures, on the other hand, saturate at about 35 e⁻/s and evidence can be seen of pixels hotter

than this in the STIS data. Details of the superdark production and hot pixels identification can be found in Mutcher, *et al.*¹³ Weekly superdark images exist for STIS from shortly after installation in HST on 14 February 1997 until the present and are publicly available from the Multi-mission Archive at Space Telescope (MAST). Daily superdarks exist for ACS/HRC from 1 March 2002, after installation in February 2002, until the present.

Accumulating radiation damage in the CCDs constantly increases the number of hot pixels so the HST instruments heat their CCDs to temperatures between 5C and 20C for several hours each month to anneal the accumulated damage and reduce the number of hot pixels. For purposes of examining hot pixel behavior these anneals break the hot pixel data into periods of about 1 month length in which undisturbed hot pixels can be analyzed. We selected the sets of superdark images given in Table 2 from ACS/HRC and STIS to sample the full length of each instrument’s exposure to radiation.

| ACS/HRC | | STIS | | |
|-------------------------|----------------------------|-----------------------|-----------------------------|-----------------------|
| Anneal Pair | Number of daily superdarks | Anneal Pair | Number of weekly superdarks | Note |
| 26 April 02 – 22 May 02 | 23 | 17 May 97 – 20 Jun 97 | 5 | |
| 19 May 03 – 21 Jun 03 | 33 | 17 Jun 98 – 10 Aug 98 | 7 | Missed monthly anneal |
| 19 Jul 03 – 14 Aug 03 | 24 | 4 May 99 – 13 Jun 99 | 5 | |
| 1 Dec 03 – 3 Jan 04 | 33 | 24 Oct 99 – 11 Jan 00 | 5 | Service mission 3 |
| | | 27 Aug 01 – 23 Sep 01 | 4 | |
| | | 19 Mar 02 – 18 Apr 02 | 4 | |

Table 2. Data sets from ACS/HRC and STIS used for analysis.

3.2 WFPC2

The WFPC2 instrument maintains lists of weekly hot pixel data compiled between anneals from 5 dark frames taken each week. The lists include, for each hot pixel in each of the 4 CCDs, weekly dark currents, the minimum, maximum, average, and rms variation of the weekly currents. Hot pixels are identified if their dark current exceeds 5σ above the average for their CCD, or the rms variation of their dark current exceed 4 times the rms variation for their CCD, or their maximum dark current exceed a fixed value, or if the peak to peak variation in their dark current exceeds a fixed value.

| Anneal pair | Number of weekly samples |
|-----------------------|--------------------------|
| 24 Jul 97 – 20 Aug 97 | 6 |
| 30 Dec 00 – 23 Jan 01 | 5 |
| 5 Dec 03 – 12 Feb 03 | 12 |

Table 3. WFPC2 hot pixel lists used

4. ANALYSIS AND RESULTS

4.1 ACS/HRC

Hot pixel statistics for the four sets of ACS/HRC data are given in Table 4. These data cover 20 months of operation starting shortly after the installation of ACS in February 2002. Recall that each set is a time series of daily samples of dark current for pixels that were found hot in any sample of the time series. The first column identifies the data set by start date. Column two gives the range of the bins for the statistics in the following columns. Values in the table give the number of pixels out of the 1024x1024 array that fall within the bin in column two for each of the statistics in columns 3 through 8. The total line sums the pixel numbers to give the total number of pixels that were hotter than $2 e^-/s$ for any sample in the data set. A histogram of the pixels hotter than $2 e^-/s$ in the data set starting 1 Dec 2003 is shown in Figure 1. The number of hot pixels is seen to drop rapidly up to about $6 e^-/s$ and the distribution shows no effects of saturation.

The “max” statistic in column three is simply the maximum value of a pixel over all samples of the time series. By definition there are no max values less than 0.5σ . The peak to peak variation over the data set is reported in column four as “max-min”. The maximum positive difference and minimum negative difference statistics of columns 5 and 6 were compiled from the difference between all samples but the first and their preceding samples. Columns 7 and 8 give the number of responses, or “rings”, of a (-0.5,1,-0.5) filter kernel run along the time series.

The peak to peak variation gives a general indication of the activity of the hot pixels but has no direct connection to Kepler noise since the separation in time of the extrema is not specified. The maximum positive and

minimum negative differences are more relevant to Kepler since the difference between daily values measure a time scale within a factor of 2 of the time scales of importance to Kepler. The rapid excursions picked out by the difference extrema will add noise to the Kepler transit detection statistics but by themselves won't necessarily mimic a transit since the transition in one direction is not usually followed immediately by a transition in the other direction. There are always more positive differences than minimum negative differences. This is due to the characteristically faster rise time (1 to 2 days) than fall time (several days, if they decay at all) of the hot pixel variations. These rates of rise and decay are generally consistent with measurements of random telegraph noise (RTS) in room temperature irradiated CCDs and the observation that the time scale for RTS fluctuations increases at low temperatures^{14,15}. The number of filter rings is the most significant to predicting hot pixel effects on Kepler since these do pick out transitions in one direction followed immediately by an opposite transition. The filter response statistics estimate, to within the uncertainty associated with the difference in time scales, the number of times a false transit due to hot pixel variation might actually be detected. Only negative rings could be mistaken for planetary transits. Note that the number of negative rings is approximately 2 per month at $>1\sigma$ for the entire 1024x1024 array.

| Start Date | | max | max - min | max positive difference | min negative difference | positive rings | negative rings |
|---------------|-----------|-----|-----------|-------------------------|-------------------------|----------------|----------------|
| 26 April 2002 | < 0.5 _ | 0 | 24 | 34 | 59 | - | - |
| | 0.5 - 1 _ | 32 | 22 | 18 | 10 | 4 | 2 |
| | 1 - 4 _ | 35 | 22 | 17 | 4 | 1 | 1 |
| | > 4 _ | 7 | 6 | 5 | 1 | | |
| | Total | 74 | | | | | |
| 19 May 2003 | < 0.5 _ | 0 | 170 | 202 | 234 | - | - |
| | 0.5 - 1 _ | 140 | 51 | 33 | 19 | 6 | 1 |
| | 1 - 4 _ | 100 | 32 | 20 | 3 | 2 | 3 |
| | > 4 _ | 17 | 4 | 2 | 1 | | |
| | Total | 257 | | | | | |
| 19 July 2003 | < 0.5 _ | 0 | 202 | 220 | 245 | - | - |
| | 0.5 - 1 _ | 131 | 32 | 20 | 9 | 5 | 0 |
| | 1 - 4 _ | 112 | 22 | 18 | 5 | 5 | 1 |
| | > 4 _ | 16 | 3 | 1 | 0 | | |
| | Total | 259 | | | | | |
| 1 Dec 2003 | < 0.5 _ | 0 | 231 | 255 | 289 | - | - |
| | 0.5 - 1 _ | 170 | 46 | 32 | 17 | 4 | 1 |
| | 1 - 4 _ | 121 | 34 | 25 | 8 | 2 | 2 |
| | > 4 _ | 24 | 4 | 3 | 1 | | |
| | Total | 315 | | | | | |

Table 4. Hot pixel statistics for ACS/HRC. The meanings of the statistics in columns 3 – 8 are discussed in the text. Values are the number of pixels. $1\sigma = 4 \text{ e-/s}$

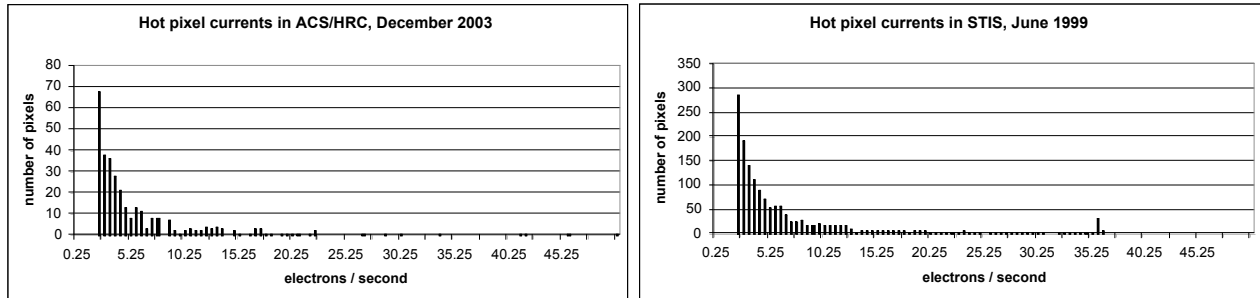


Figure 1. Histograms of the hot pixel currents above 2 e/s for samples of ACS/HRC and STIS data.

The number of potentially troublesome hot pixels in the ACS/HRC detector clearly grew significantly over the 20 month period covered by Table 4. The number of post anneal pixels hotter than $2 \text{ e}^-/\text{s}$ grew fairly steadily at an average of 0.4 pixels per day. The growth rate between anneals was fairly steady at 2 pixels/day with each anneal removing about 80% of the new hot pixels. This is consistent with the $\sim 80\%$ anneal rate reported for all hot pixels¹⁶.

4.2 STIS

The STIS hot pixel data sets are similar to the ACS/HRC data. The principal differences are the longer exposure period of STIS to the space environment, 5 years as opposed to 20 months for ACS, and the longer sampling period of 1 week. The STIS data were treated in the same way as the ACS/HRC data except that, due to the coarse sampling interval, the simple transit detection filter was not used. Rather than tabulate the STIS results we will discuss them in contrast to the ACS/HRC.

The general character of the STIS hot pixel distribution is similar to but more numerous than the ACS/HRC distribution. The histogram of STIS hot pixels from the June 1999 data in Figure 1 has much the same shape as the ACS/HRC histogram but with more hot pixels and a somewhat more populated high current tail. The effect of saturation in the STIS electronics can be seen as the spike near $36 \text{ e}^-/\text{s}$. The similarity of the STIS and ACS/HRC distributions and the fact that the CCDs in the two instruments are nominally identical argues that the hottest pixels in STIS are no hotter than the maximum of $60 \text{ e}^-/\text{s}$ found in ACS/HRC.

For months 3 through 20 of each instrument's radiation exposure life STIS displayed about 4 times more post anneal pixels hotter than $2 \text{ e}^-/\text{s}$ than did ACS/HRC. The post anneal hot count grew steadily at 1.6 pixels per day for the first 2.2 years of STIS's life and then appeared, from this analysis, to average 0.6 pixels per day through year 5. An anomalously high number of post anneal hot pixels appeared in the 24 October 1999 data set and no data was analyzed here for the next 1.8 years. Note that the HST servicing mission number 3 occurred at the time of this anomaly. During its first 3 years STIS acquired about 5 pixels per day hotter than $2 \text{ e}^-/\text{s}$ in between anneals after which the daily rate dropped to about 2 per day in the data analyzed. The anneals appear to reduce the hot pixel counts by about 70%. This behavior is consistent with reports by the STIS team¹⁷ except that our analysis gets a somewhat higher anneal rate for the hottest pixels.

Due to the week long sampling interval of the STIS dark data the only useful statistic on the variability of $>2 \text{ e}^-/\text{s}$ hot pixels is the maximum-minimum over the intra-anneal periods. STIS generally displayed 2-4 times as many 1-4_ max-min pixels as did ACS/HRC and 2-6 times as many >4 _ max-min pixels. Two intra-anneal periods were notable exceptions. During the period starting in June 1998 the >4 _ max-min pixel count was 13 times the average ACS/HRC number while the 1-4_ count was only 2 times elevated. During the period starting in October 1999 STIS had 14 and 29 times higher 1-4_ and >4 _ max-min counts. With the exception of these unusual intra-anneal periods the STIS statistics appeared to be well behaved at a level 2-6 times higher than ACS/HRC.

4.3 WFPC2

The WFPC2 hot pixel data were selected for pixels hot enough to be of interest to Kepler similarly to the data from ACS/HRC and STIS. The time series between anneals were used to calculate the maximum-minimum statistic to find the number of pixels that could possibly cause trouble for Kepler. At most 70 pixels in each of the four 800×800 CCDs had maximum dark currents above $2 \text{ e}^-/\text{s}$ in all three of the data sets. At most 9 pixels in any CCD showed a peak to peak variation greater than $2 \text{ e}^-/\text{s}$. The highest dark current listed in the WFPC2 data was $15 \text{ e}^-/\text{s}$. Naively scaling these counts by area from WFPC2's 800×800 arrays of $17 \mu\text{m}$ pixels to ACS/HRC's 1024×1024 array of $21 \mu\text{m}$ pixels indicates that, compared to the average values of ACS/HRC, WFPC2 had about 30% fewer pixels hotter than $2 \text{ e}^-/\text{s}$. Of those hotter pixels, about 11% were variable at the $2 \text{ e}^-/\text{s}$ level compared to 20% for ACS/HRC.

The general characteristics of the WFPC2 hot pixel behavior are similar to, and perhaps somewhat more benign than those of ACS/HRC and STIS.

- 1) No WFPC2 pixel ever displayed a dark current of more than $15 \text{ e}^-/\text{s}$. This is just enough to mimic a significant transit if the current varies by its full amplitude with the proper transit signature.
- 2) Most of the hotter hot pixels have very stable dark currents, far below a variability of 0.5σ for Kepler.
- 4) A very few pixels do vary, apparently randomly by enough to exceed 0.5σ . Another very few pixels are seen to spontaneously turn on and even turn off with current changes large enough to exceed 0.5σ .
- 5) The number of potentially offensive hot pixels increased modestly over the years between 1997 and 2003.

While the large differences in CCD construction make WFPC2 a poor model for Kepler CCD performance, the WFPC2 hot pixel behavior would be no worse for Kepler than that of ACS/HRC or STIS and lends some confidence to conclusions drawn from their data.

5. EFFECTS ON KEPLER

Assuming that the number of damage centers that cause hot pixels goes as the volume of the detector we can conservatively scale the number of hot pixels seen in ACS/HRC by the ratio of the total number of pixels, the ratio of pixel areas, $(27/21)^2 = 1.65$, between ACS/HRC and Kepler and the factor of 3.3 for DDD derived in section 1.2. This assumes that there is at most one damage center per pixel and ignores any differences in effective pixel depth between ACS/HRC and Kepler. The depletion depths of the CCDs are similar enough that real differences are uncertain. The expected ratio of hot pixels to total pixels in Kepler is then the ACS/HRC value times $3.3 \times 1.65/1024^2$. Kepler will monitor about 1×10^5 stars using an average of about 30 pixels for each star, 3×10^6 total pixels. We will pick the 19 May 2003 data set from ACS/HRC and scale the counts by $3 \times 10^6 \times 3.3 \times 1.65/1024^2$ to get an estimate of the number of troublesome pixels expected in Kepler data. The scaled counts are shown in the upper rows of Table 5. A correction for the lower operating temperature of Kepler, using the histogram of the 19 May HRC data, is made in the lower rows of Table 5.

| Predicted Kepler hot pixel counts | | max - min | max positive difference | min negative difference | positive rings | negative rings |
|-----------------------------------|-----------|-----------|-------------------------|-------------------------|----------------|----------------|
| -81C | 0.5 - 1 _ | 790 | 515 | 300 | 90 | 16 |
| | 1 - 4 _ | 500 | 313 | 45 | 30 | 45 |
| | > 4 _ | 60 | 30 | 16 | 0 | 0 |
| -93C 5x less current | 0.5 - 1 _ | 16 | 10 | 3 | | |
| | 1 - 4 _ | 10 | 3 | 3 | | |
| | > 4 _ | 0 | 0 | 0 | | |

Table 5. Hot pixel statistics from ACS/HRC 19 May 2003 data scaled to the Kepler pixel size, number of active pixels and displacement damage dose. The top 3 rows assume operation of the Kepler CCD at the same temperature as ACS/HRC. The bottom three rows give the predicted counts for operation at -93C which will reduce dark currents by about a factor of 5.

Before correction for operating temperature hot pixels could be noticeable at the few σ level for as many as 560 stars and could raise the noise level, at times, for another 790 or so. Using the filter ring rate as a measure of how often trouble might occur, about 45 stars might produce a transit-like, negative ring, signal above 1σ once each month. This is a very small number of false transit signals. Random noise on 100,000 stars will produce about 20,000 3σ and 400 4σ events each month. Recall that Earth would produce a 4σ transit. After correcting for the operating temperature of the Kepler CCDs there should be sensibly no transit-like events due to hot pixel variation. These transit filter ring rate estimates refer to a time scale of 24 hours but should be applicable to the Kepler time scale of 6 – 13 hours so long as the power spectrum of the hot pixel variations does not increase much at shorter time scales. Since the rate of variation on active hot pixels is seen to be on the order of a day or two there is no reason seen in this data to expect fluctuation to increase in amplitude with shorter time scales.

Even if some hot pixel induced transit-like events do appear, the Kepler planet search algorithm will require that they match a series of other transit event candidates with amplitude precision consistent with their noise and timing precision consistent with the periodicity of a planetary orbit. This timing and amplitude precision filter is designed to cope with the 400 4σ random false transit events per month and allow at most one false positive planetary detection over the Kepler mission.

A further filter is applied to transit-like events in the form of an examination of the individual levels of the pixels associated with each star during a transit-like event. All of the pixels must dim proportionally to their signal during a transit. A single hot pixel varying within the star's pixel group will be easily seen and the transit-like event rejected.

We expect Kepler will have no problems with hot pixels at the level predicted from the ACS/HRC detector. However, the hot pixel counts actually seen by Kepler could be substantially larger. The STIS CCD gained un-annealable hot pixels at an average rate 2.4 times faster than ACS/HRC and Kepler does not currently plan to anneal

as frequently as the HST instruments do. Considering its low operating temperature Kepler will tolerate factors of a few more hot pixels than ACS/HRC, similar to the numbers displayed by STIS. Kepler will have the opportunity to anneal its CCDs every 90 days, if required. If Kepler's hot pixel growth rate is similar to that of ACS/HRC and the Kepler detectors are annealed every 90 days the hot pixel count at the end of the nominal 4 year mission will be about 1.5 times that seen in the ACS/HRC data of 19 May 2003, accounting for 3x increase due to the longer anneal interval, 3.3x increase for the extra DDD and a factor of 6.6 decrease for the colder temperature of the Kepler CCDs. This should be a tolerable level and will probably still be tolerable if increased again by a factor of 2.4 to account for STIS-like growth rates. If Kepler does not ever anneal its detectors the end of mission hot pixel counts will be 5.5 times higher than ACS/HRC on 19 May 2003 and possibly 13 times higher. The effects of such high levels of hot pixel counts are difficult to assess but are certainly of a magnitude that Kepler will have to track carefully. The Kepler data processing system is preparing to track the number and effects of hot pixels and will be able to recommend anneal procedures when needed. A mitigating feature of the Kepler orbit is that in helio-centric orbit the radiation dose tends to arrive in bursts coincident with high solar activity. Fewer, less frequent anneals may be needed than in the case of low earth orbits where radiation exposure is fairly constant from orbit to orbit. Kepler plans to launch near solar minimum and its nominal mission should be over before the next solar activity peak. Kepler may get little radiation dose during the first half of its life and perhaps fairly mild radiation exposure thereafter.

ACKNOWLEDGMENTS

This work was supported by the NASA Discovery program under task order NMO-710711. The authors would like to thank Jim Janesick of the Sarnoff Corporation, Rob Philbrick and Neal Nickles of Ball Aerospace and Technologies Corporation and Jon Jenkins of the SETI Institute for helpful comments and discussions.

REFERENCES

1. Kock, D. G., W. Borucki, E. Dunham, J. Jenkins, L. Webster, and F. Witteborn, "CCD photometry tests for a mission to detect Earth-size planets in the extended solar neighborhood", *UV, Optical and IR Space Telescopes and Instruments*, Breckenridge, J. B., Jakobsen, P.; Eds., Proc. SPIE vol. 4013, pp. 508-519, SPIE, 2000.
2. Borucki, William J.; *et al.*, "Kepler Mission: a mission to find Earth-size planets in the habitable zone", *Proceedings of the Conference on Towards Other Earths: DARWIN/TPF and the Search for Extrasolar Terrestrial Planets*, 22-25 April 2003, Heidelberg, Germany, M. Fridlund, T. Henning, Eds.; ESA SP-539, p. 69, ESA Publications Division, Noordwijk, Netherlands: 2003.
3. Kock, D., *et al.*, "Overview and status of the Kepler Mission", *Optical, Infrared and Millimeter Space Telescopes*, Proc. SPIE vol. 5487 (this volume), 2004.
4. Jenkins, J. M., *et al.*, "Processing CCD images to detect transits of Earth-sized planets: Maximizing sensitivity while achieving reasonable downlink requirements", *UV, Optical, and IR Space Telescopes and Instruments*, Breckenridge, J. B., Jakobsen, P.; Eds., Proc. SPIE vol. 4013, pp. 520-531, SPIE, 2000.
5. Personal communication. Rob Philbrick, Ball Aerospace and Technologies Corporation, 2004.
6. Hopkinson, G.R., Dale, C.J. and Marshall, P.W., "Proton Effects in Charge-Coupled Devices", *IEEE Transactions on Nuclear Science*, **43**, p. 614, 1996.
7. Nickles, N., "Kepler Sector Analysis for CCD Radiation Specification", System Engineering Report Kepler-SER-SYS-019, Ball Aerospace and Technologies Corporation, 2002.
8. Feaver, D., "WFC CCD Radiation Shielding Analysis", System Engineering Report ACS-CCD-019, Ball Aerospace and Technologies Corporation, 1997.
9. Feaver, D., "HRC CCD Radiation Shielding Analysis", System Engineering Report ACS-CCD-020, Ball Aerospace and Technologies Corporation, 1997.
10. Jones, M. R., "ACS WFC CCD Radiation Test: The Radiation Environment", Instrument Science Report ACS-2000-09, Space Telescope Science Institute, 2000.
11. Dale, C., *et al.*, "Displacement Damage Effects in Mixed Particle Environments for Shielded Spacecraft CCDs", *IEEE Transactions on Nuclear Science*, **40**, p. 1628, 1993.
12. Bohlin, R. and Goudfrooij, P., "An Algorithm for Correcting CTE Loss in Spectrophotometry of Point Sources with the STIS CCD", Instrument Science Report STIS 2003-03R, Space Telescope Science Institute, 2003.
13. Mutcher, M., Riess, A. and Van Orsow, D., "Bias and dark calibration of ACS data", Instrument Science Report ACS 2004-DRAFT, Space Telescope Science Institute, 2004.

14. Hopkins, I.H. and Hopkinson, G.R., "Further measurements of random telegraph signals in proton irradiated CCDs", IEEE Transaction on Nuclear Science, **42**, pp. 2074-2081, 1995.
15. Hopkinson, G.R. and Mohammadzadeh, A., "Comparison of CCD Damage due to 10 and 60 MeV protons", Presentation at the IEEE 2003 NSREC, Monterey, CA., July 2003.
16. Riess, Adam, et al., "A First Look at Hot Pixels on ACS", Instrument Science Report ACS 2002-06, Space Telescope Science Institute, 2002.
17. Hayes, J. J. E., Christensen, J. A. and Goudfrooij, P., "STIS CCD Anneals", Instrument Science Report STIS 1998-06 Rev A, Space Telescope Science Institute, 1998.